Cemef

Centre de Mise en Forme des Matériaux

Mines Paris - PSL

CNRS UMR 7635

Sophia Antipolis, France

Self-supervised machine learning of ROM-nets for mechanics of materials

D. Ryckelynck

Y. Maday's Chair Collège de France June 22-24 2026

The naive use of IA is likely to be a high-risk strategy

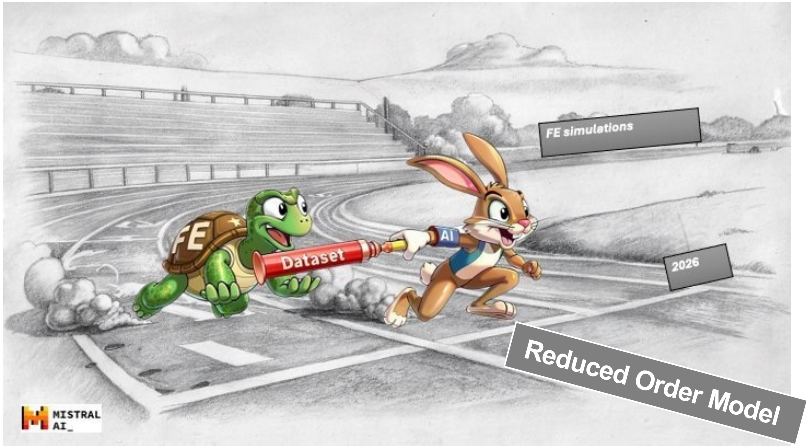

Now it's time to collaborate!

- **R1**: Loss of human expertise: This risk can be avoided by developing **reduced order model** as a downstream model after self-supervised machine learning task..

- **R2**: Undetected bias and errors:
  Without **human expertise** to validate and interpret predictions, critical errors could have serious consequences. It is important to continue training experts in mechanics of materials with strong AI skills.

- **R3**: Excessive standardization, especially for data from industry: We propose **Physics-based simulations** to create synthetic datasets for self-supervised machine learning.

INTEGRATING PHYSICS-BASED MODELING WITH AI

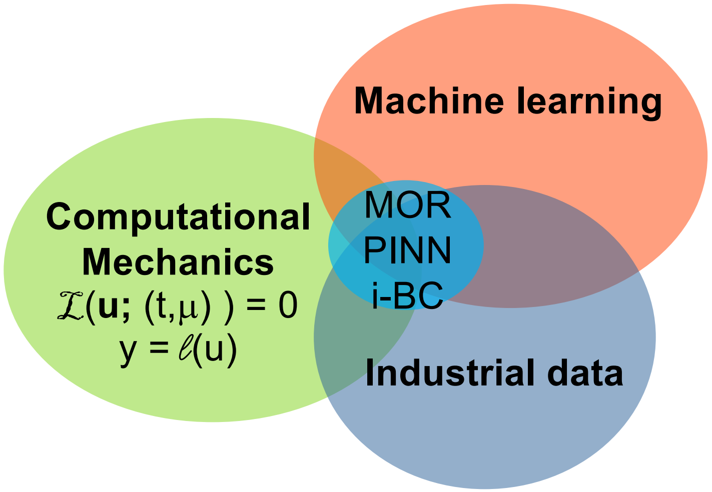

Jared Willard, Xiaowei Jia, Shaoming Xu, Michael Steinbach, Vipin Kumar (2022).
Integrating Scientific Knowledge with Machine Learning for Engineering and Environmental Systems. arXiv

IA

Machine Learning

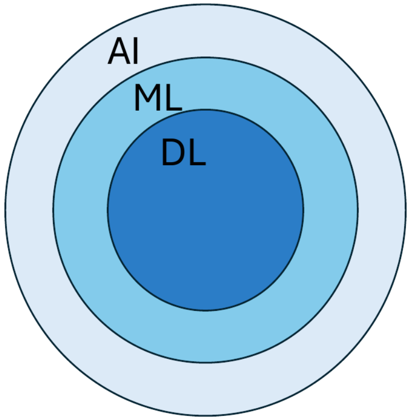

Main caterogies:

- Supervised machine learning**, Y(X) based on examples** (X,Y)
- Unsupervised machine learning based on X (clustering, OOD...).
- **Self-supervised machine learning, Y = X for pretrained models, dimensionality reduction task, masking strategies***
- Reinforcement learning, optimization, autonomous systems...
- Model adaptation (fine-tuning, transfer learning…)

Scientific Machine learning

- Intelligent surrogate modeling (regression task $\mu \rightarrow$ y, or $\mu \rightarrow$ u $\rightarrow$ y)
- Physics Informed Neural Networks
- **Projection-Based Model Order Reduction, hyperreduction**
- **Intelligent boundary conditions**
- Neural ODE…
- Thermodynamics-based Artificial Neural Networks (TANN) …

Pretrained and donwstream models strategy

*extension of the Gappy POD

Synthetic data for pretrained model

Implementation steps in compuational mechanics :

- Choose a parametric Finite Element Model

- Choose an ambient space for data
- Save **datasets**
- **Augment data** in the train dataset

- Choose a neural network **architecture** and a **loss**

- **Train** a pretrained model without overfitting
- **Test** the pretrained model

- **Adapt** the pretrained model to a specific task, like intelligent surrogate modeling or projection-based model order reduction or intelligent boundary condition setting

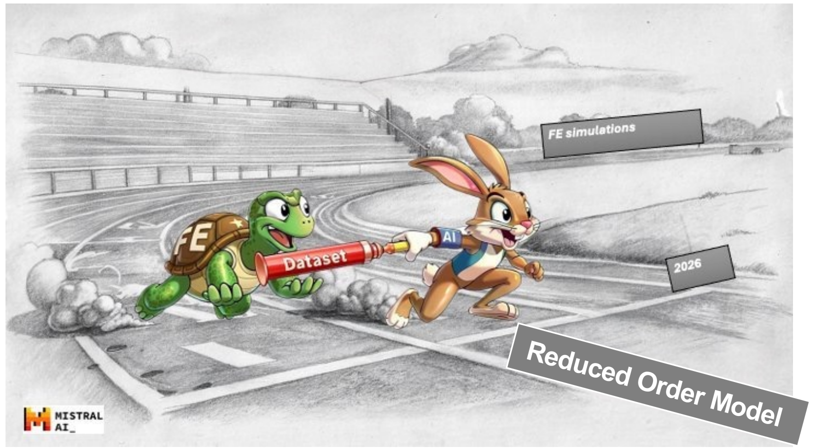

Numerical example: void modeling in dilution condition and linear elasticity

$\mathbf{u} \in \mathcal{H}_0(\Omega)+\boldsymbol{u}_D$ local affine space parametrized by an image.

$\mathcal{L}(\mathbf{u}; (t,\mu))$ is linear with respect to boundary conditions and some material coefficients.

Nonlinear with respect to the shape of the domain Ω.

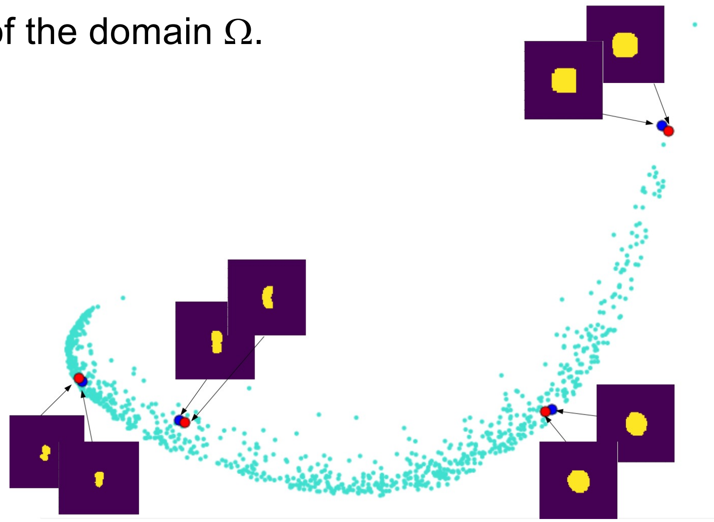

3D latent space

H. Launay's PhD

Motivations

Learning **intelligent boundary conditions** on $\partial\Omega$, where Ω is a variable
(as an extension of Reduced Integration Domain in Hyper-reduction [Ryckelynck 2016])

Learning a **Grassmann manifold** Gr(k,n; Ω) in computer vision for model order reduction [Nguyen 2018].

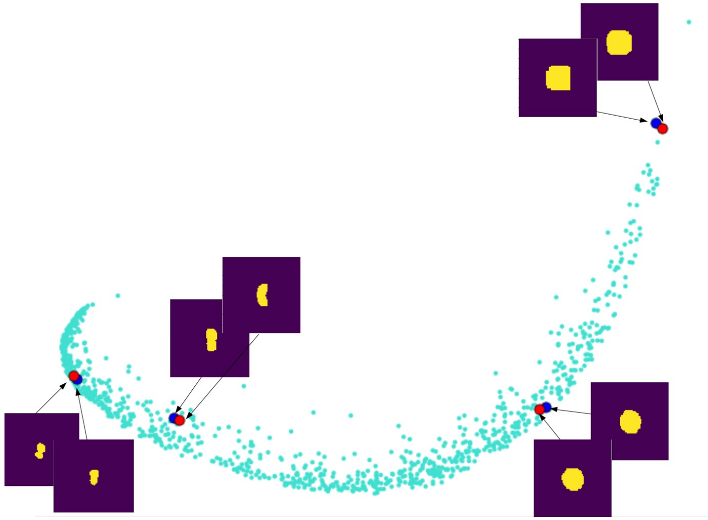

H. Launay's PhD

[Ryckelynck 2016] Hyper-reduced predictions for lifetime assessment of elasto-plastic structures D Ryckelynck, K Lampoh, S Quilicy
Meccanica 2016, 51 (2), 309-317
[Nguyen 2018] Computer vision with error estimation for reduced order modeling of macroscopic mechanical tests F Nguyen, SM Barhli, DP Muñoz, D Ryckelynck
Complexity 2018 (1), 3791543

Numerical example: void modeling in dilution condition and linear elasticity

Xindus = Image of a defect (48x48x1 tensor) from X-ray Tomography,
Y = 3 strain fields of 3 components related to 3 macroscopic loading

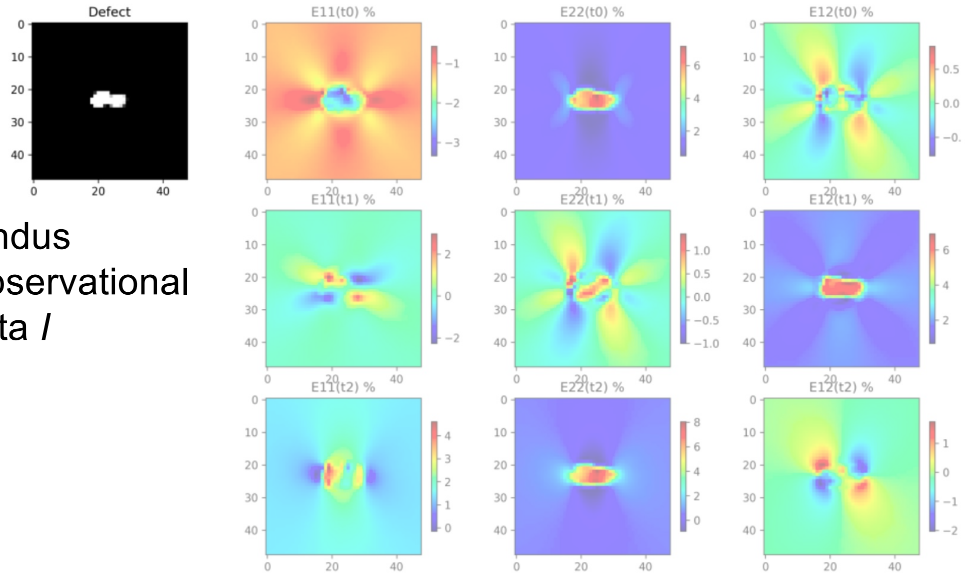

Xindus
Observational
data *I*

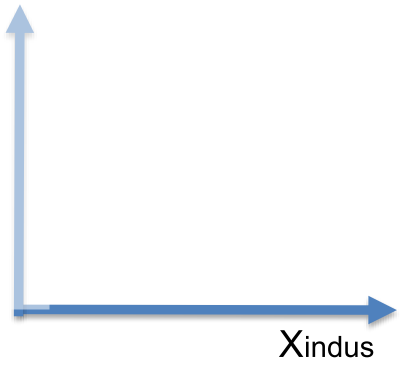

Numerical example: void modeling in dilution condition and linear elasticity

Xindus = Image of a defect (48x48x1 tensor),
Y = 3 strain fields of 3 components related to 3 macroscopic loading (BC1, BC2, BC3)

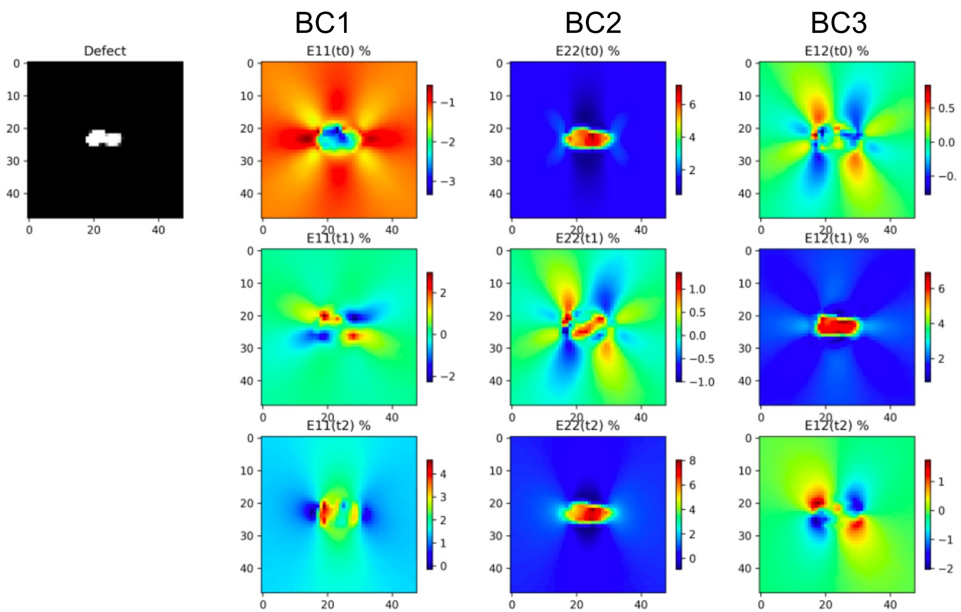

Snapshots (I-surrogate or i-BC)
Y: 9 strain fields

Local reduced basis of dimension 3
$Y \in Gr(3,n)$, $n = 46 \times 46$

Train a digital twin for strain prediction or reduced-basis prediction

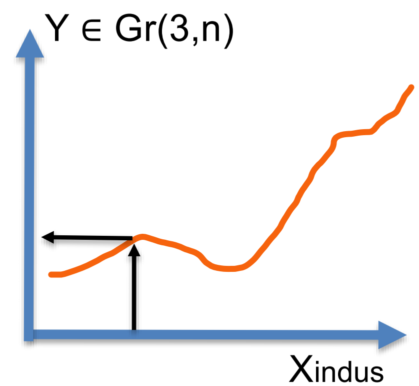

L. Lacourt's PhD

Update the loss !

Theory: void modeling in dilution condition and elasticity

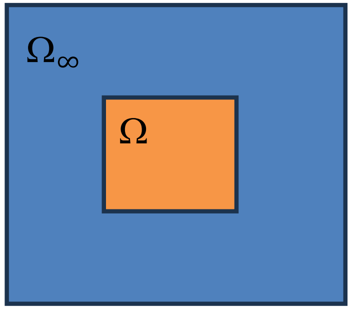

Domain for dilution condition
Local PB HROM
i-BC for submodel

$$div(\, \boldsymbol{C}(\boldsymbol{x})\, \varepsilon(\boldsymbol{u})\,) = f \quad \forall x \in \Omega, \qquad \boldsymbol{u}(x) = \boldsymbol{u}_D(x) \;\; \forall x \in \partial\Omega$$

$$\boldsymbol{v} \in V, \qquad V = \{v \in H^1(\Omega), \boldsymbol{v}(x) = \boldsymbol{u}_D(x) \;\; \forall x \in \partial\Omega\}$$

Ellipticity
$$\alpha_\Omega \, \|\boldsymbol{v}\|_\Omega{}^2 \;\le \int_\Omega tr\big(\varepsilon(\boldsymbol{v})\, \boldsymbol{C}\, \varepsilon(\boldsymbol{v})\big)\, d\Omega \;\le\; \gamma_\Omega \; \|\boldsymbol{v}\|_\Omega{}^2$$

Coercivity $\alpha_{\Omega,} > 0$

Continuity $\gamma_{\Omega,} > 0$

Computer vision tasks :

$$I \;\rightarrow\; \Omega(\mathrm{I}), \boldsymbol{Y}(\mathrm{x}; \mathrm{I}), \boldsymbol{u}_D(\mathrm{x}; \mathrm{I}) \quad x \in \Omega(I)$$

Y for projection-based Model Order Reduction using Hyperreduction (PB HROM)
$\boldsymbol{u}_D(\mathrm{x}; \mathrm{I})$ for intelligent boundary condition.

Theory: void modeling in dilution condition and linear elasticity

$$div(\,\boldsymbol{C}(\boldsymbol{x})\,\varepsilon(\boldsymbol{u})\,) = f \quad \forall x \in \Omega, \qquad \boldsymbol{u}(x) = \boldsymbol{u}_D(x) \;\; \forall x \in \partial\Omega$$

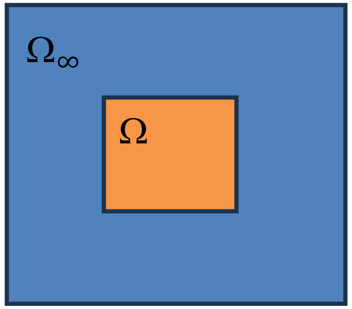

Domain for dilution condition

FE modeling : ***Kq = F***

$$\boldsymbol{u_N}(x;I) = \boldsymbol{E}\,x + \sum_{i=0}^{N} \boldsymbol{\varphi}_i(x;I)\;\; q_i(I) + \;\boldsymbol{r}\big(\boldsymbol{u}_D(I)\big)$$

macro strain
+ dof fluctuation
+ filting of boundary condition

$$K_{ij}(x;I) = \int_{\Omega(\mathrm{I})} tr\left(\varepsilon(\boldsymbol{\varphi}_i)\;\boldsymbol{C}(\boldsymbol{x};\boldsymbol{I})\;\varepsilon\big(\boldsymbol{\varphi}_j\big)\right)\, d\Omega$$

$$\tilde{\alpha}\;\|\boldsymbol{q}\|_2{}^2 \leq \;\boldsymbol{q}^T\boldsymbol{K}\;\boldsymbol{q} \;\leq\; \tilde{\gamma}\;\|\boldsymbol{q}\|_2{}^2$$

$$F_i(I) = -\int_{\Omega(\mathrm{I})} tr\left(\,\varepsilon(\boldsymbol{\varphi}_i)\;\boldsymbol{C}(\boldsymbol{x};\boldsymbol{I})\;\left(\,E + \varepsilon\left(\boldsymbol{r}\big(\boldsymbol{u}_D(I)\big)\right)\right)\right) d\Omega \;\; = (\boldsymbol{F_o} + \boldsymbol{B}\boldsymbol{u}_D)_{\boldsymbol{i}}$$

Theory: void modeling in dilution condition and linear elasticity

FE modeling :

$$\boldsymbol{u_N}(x;I) = \boldsymbol{E}\,x + \sum_{i=0}^{N} \boldsymbol{\varphi}_i(x;I)\; q_i(I) + \boldsymbol{r}\big(\boldsymbol{u}_D(I)\big)$$

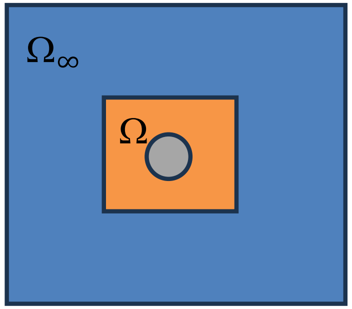

Domain for dilution condition

Zone of interest

PB ROM : Application of **Céa's lemma**

Intelligent BC (IBC) : Application of de **Saint-Venant's principle**

Hybrid model (H2ROM) : 1) PB ROM + 2) FE submodel using I-BC

Theory: void modeling in dilution condition and linear elasticity

FE modeling :

$$\boldsymbol{u_N}(x;I) = \boldsymbol{E}\,x + \sum_{i=0}^{N} \boldsymbol{\varphi}_i(x;I)\ q_i(I) + \boldsymbol{r}\big(\boldsymbol{u}_D(I)\big)$$

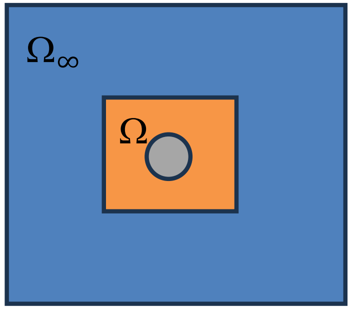

Domain for dilution condition

Zone of interest

PB ROM : Application of **Céa's lemma**

$$\boldsymbol{u} \in V, \boldsymbol{u_n} \in V_n, \boldsymbol{v_n} \in V_n, V_n \subset V_N \subset V$$

$$\|u - u_n\| \leq \frac{\gamma_\Omega}{a_\Omega}\|u - v_n\| \quad \forall\, \boldsymbol{v_n} \in V_n$$

Intelligent BC (IBC) : Application of de **Saint-Venant's principle**

Hybrid model (H2ROM) : 1) PB ROM + 2) FE submodel using IBC

Theory: void modeling in dilution condition and linear elasticity

FE modeling :

$$\boldsymbol{u_N}(x; I) = \boldsymbol{E}\, x + \sum_{i=0}^{N} \boldsymbol{\varphi}_i(x; I)\ q_i(I) + \boldsymbol{r}\big(\boldsymbol{u}_D(I)\big)$$

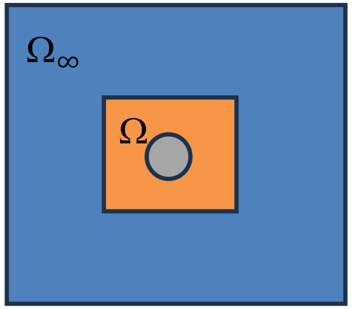

Domain for dilution condition

Zone of interest

PB ROM : Application of **Céa's lemma**

$$\boldsymbol{u} \in V, \boldsymbol{u_n} \in V_n, \boldsymbol{v_n} \in V_n, V_n \subset V_N \subset V$$

$$\|u - u_n\| \leq \frac{\gamma_\Omega}{a_\Omega} \|u - v_n\| \quad \forall\, \boldsymbol{v_n} \in V_n$$

Intelligent BC (IBC) : Application of de **Saint-Venant's principle**

Under dilution conditions, for Ω sufficiently large and far from an region of interest, the solution $\boldsymbol{u}$(x;I) is independent of $\boldsymbol{u}_D(I)$(See asymptotic properties of Green's functions [Blanc et al. 2013].). For Ω_∞, $\boldsymbol{u}_D(I)$ =0.

Hybrid model (H2ROM) : 1) PB ROM + 2) FE submodel using IBC

Theory: approximation error on a submodel using i-BC

$$\boldsymbol{u_N}(x;I) = \boldsymbol{E}\,x + \sum_{i=0}^{N} \boldsymbol{\varphi}_i(x;I)\; q_i(I) + \boldsymbol{r}\big(\boldsymbol{u}_D(I)\big)$$

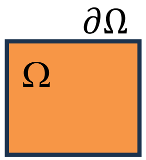

Deep learning predictions:

$\boldsymbol{u_D}_{ANN}(I)$ on $\partial\Omega$,
$\boldsymbol{r}_{ANN}(I)\ over\ \Omega$,

for FE submodel using I-BC

Error for the task of learning intelligent boundary condition

$$e_u(I) = \|\boldsymbol{u_N} - \boldsymbol{u}(\boldsymbol{r}_{ANN})\|_{\Omega}$$

$$\delta\boldsymbol{F} = \boldsymbol{F}(I) - \boldsymbol{F}_{ANN}\,, F_{ANNi}(I) = -\int_{\Omega(\mathrm{I})} tr\Big(\varepsilon(\boldsymbol{\varphi}_i)\,\boldsymbol{C}(\boldsymbol{x};\boldsymbol{I})\,\big(\boldsymbol{E} + \varepsilon\big(\boldsymbol{r}_{ANN}(I)\big)\big)\Big)\,d\Omega$$

Theory: approximation error on a submodel using i-BC

$$\boldsymbol{u}_N(x; I) = \boldsymbol{E}\, x + \sum_{i=0}^{N} \boldsymbol{\varphi}_i(x; I)\ q_i(I) + \boldsymbol{r}\big(\boldsymbol{u}_D(I)\big)$$

Convergence property for the FE submodel using IBC

$$\frac{e_u}{\|\boldsymbol{u}\|_\Omega} \leq \sqrt{\frac{\tilde{\gamma}}{\tilde{\alpha}}} \frac{\|\delta \boldsymbol{F}\|_2}{\|\boldsymbol{F}\|_2} \leq \sqrt{\frac{\tilde{\gamma}}{\tilde{\alpha}}} \frac{\|\boldsymbol{B}\|_2}{\|\boldsymbol{F}\|_2} \|\boldsymbol{u}_D - \boldsymbol{u}_{DANN}\|_{\partial\Omega}$$

The better the prediction $\boldsymbol{u}_{ANN}(I)$ on $\partial\Omega$, the better the submodel prediction.

The smaller the elements in the submodel, the larger $\tilde{\gamma}$ and the upper bound.

Data generation using a FE model

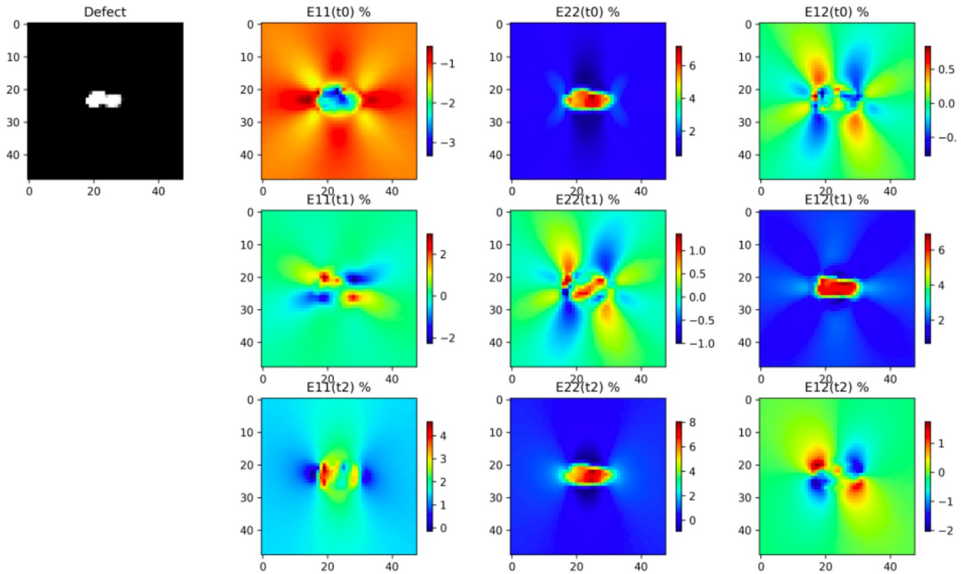

Figure 6. Strain components of the LROM for digital twin $i = 1$, on top left $\boldsymbol{\mu}_\square$, on the right $\boldsymbol{\varepsilon}(\mathbf{V}^{(1)}$.
Here, $t0$, $t1$, $t2$ stand for the indices of the vectors that span the LROM.

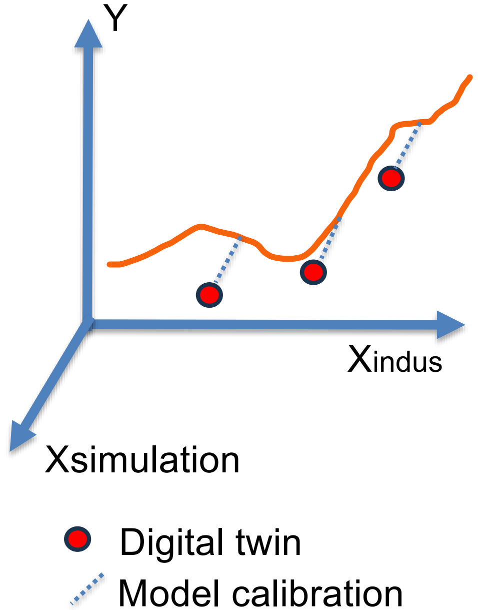

cnrs ARMINES Cemef MINES PARIS | PSL

Data augmentation

Multimodal data augmentation for digital twining assisted by artificial intelligence in mechanics of materials (2022)

HPC Computer-generated Data

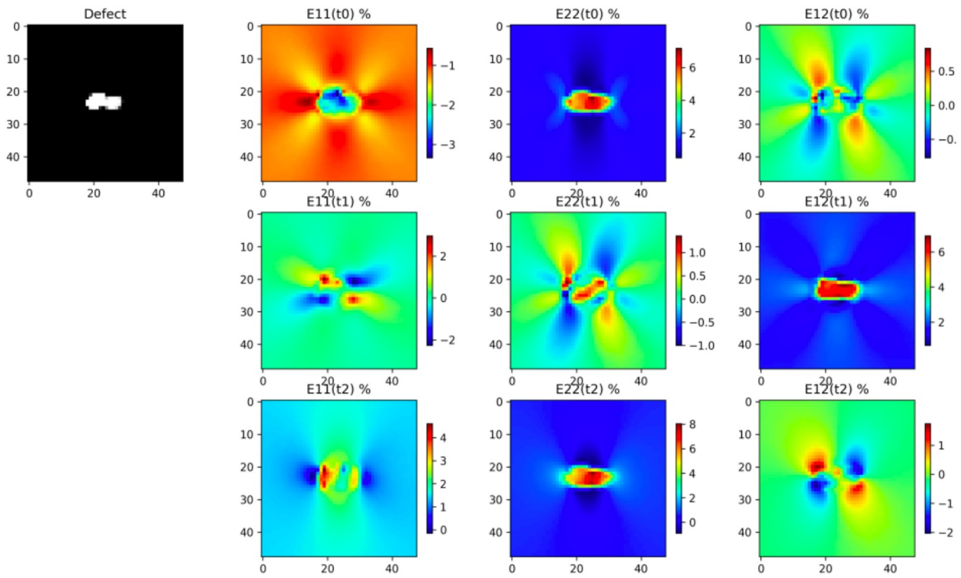

Figure 6. Strain components of the LROM for digital twin $i = 1$, on top left $\boldsymbol{\mu}_{\square}$, on the right $\boldsymbol{\varepsilon}(\mathbf{V}^{(1)}$. Here, $t0,\ t1,\ t2$ stand for the indices of the vectors that span the LROM.

A. Aublet's PhD

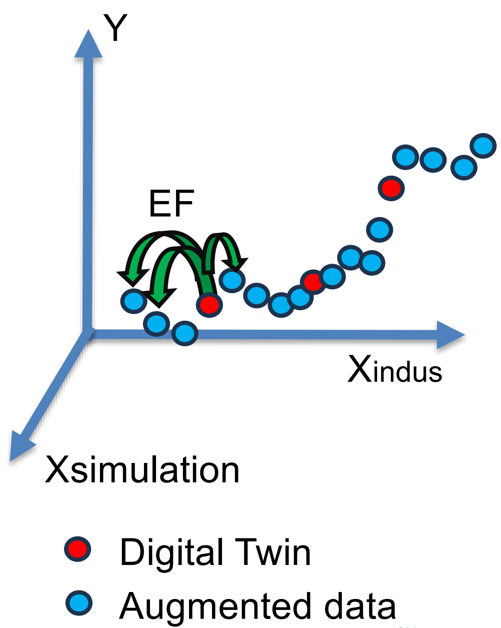

Self supervised machine learning using Autoencoder

1- For the PDE prediction

Pretrained model

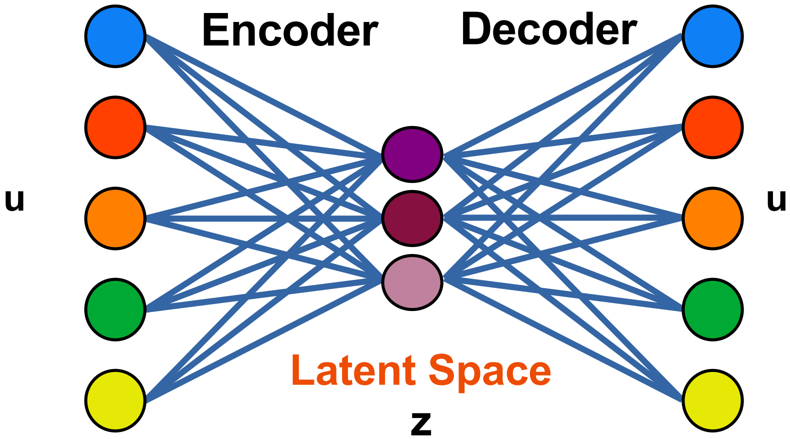

$$u \approx d_u(z)\,, \qquad z = e_u(u)$$

Selfsupervised Learning

Projection-based ROM

$$z = \underset{z*}{\operatorname{argmin}} \| \mathcal{L}(\, d_u(z\,*); (t,\mu)\,)\, \|$$

$$u_{ROM} = d_u(z)$$

K. Kashima, Nonlinear model reduction by deep autoencoder of noise response data, IEEE 55th Conference on Decision and Control (CDC) (IEEE, 2016)

Self supervised machine learning using Autoencoder

2 – Multimodal AE

Pretrained model

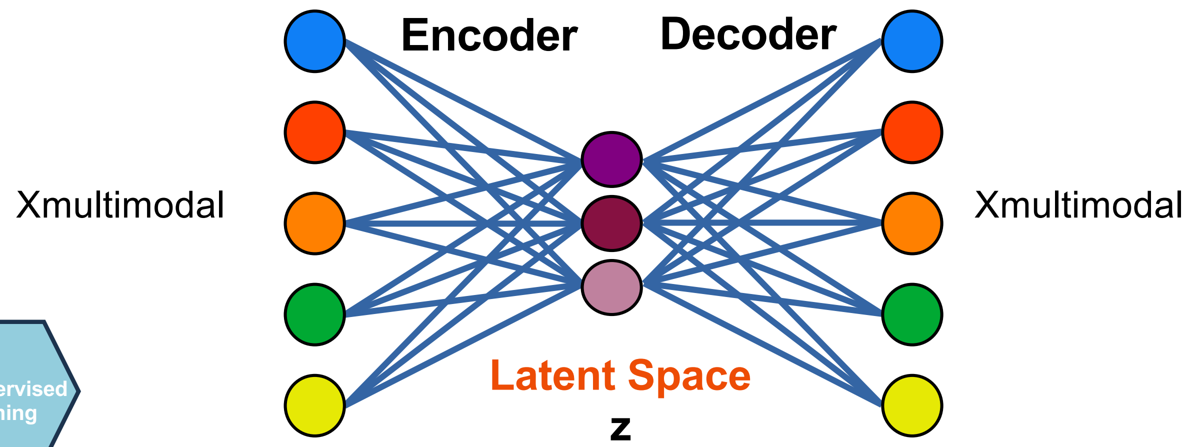

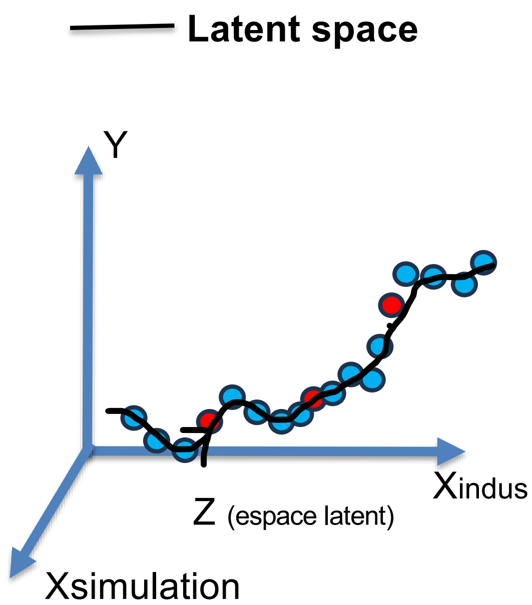

Xmultimodal = (Xindus, Xsimulation, Y)

Self supervised machine learning

Xmultimodal = (Xindus, Xsimulation, Y)

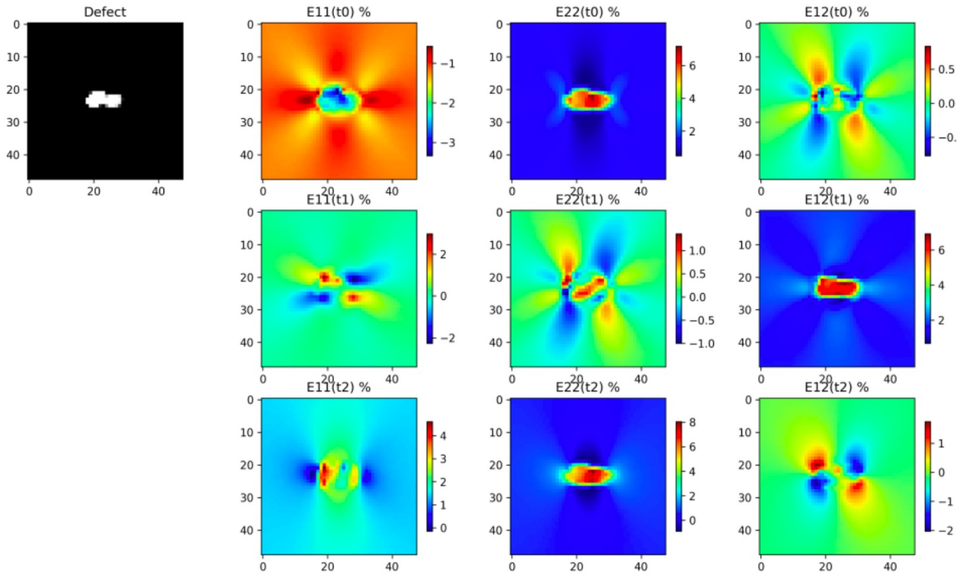

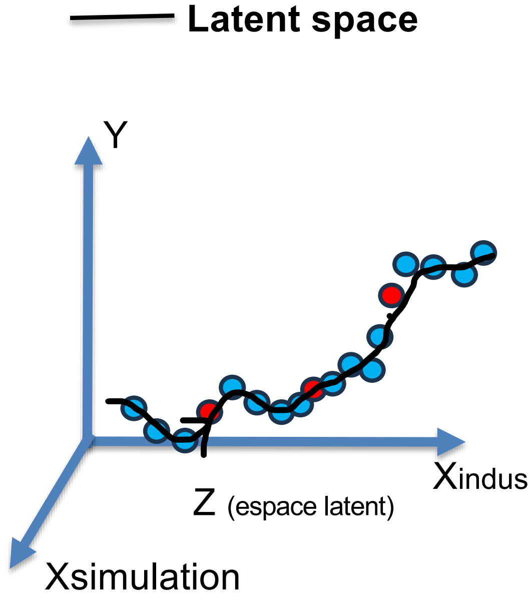

Selfsupervised Learning

Downstream task: Cross modal prediction

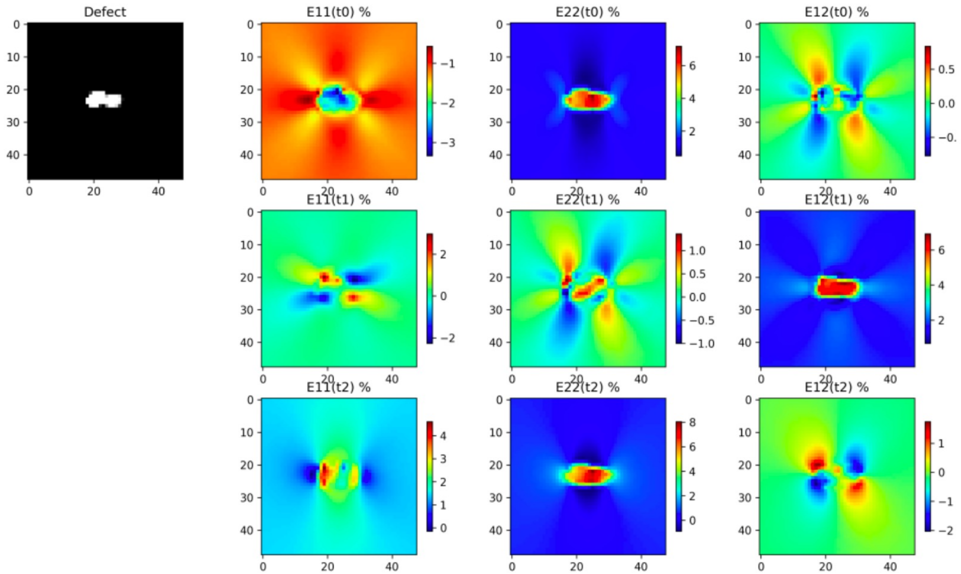

Metamodeling

Downstream tasks

- Regression task, using fine tuning. Y(Xindus).

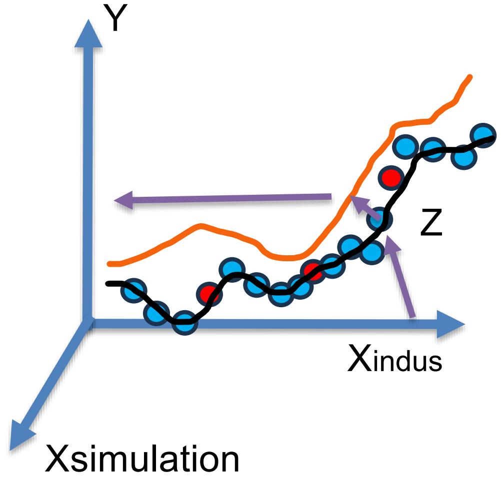

Model architecture for self-supervised machine learning on multimodal data

Dual encoder architecture

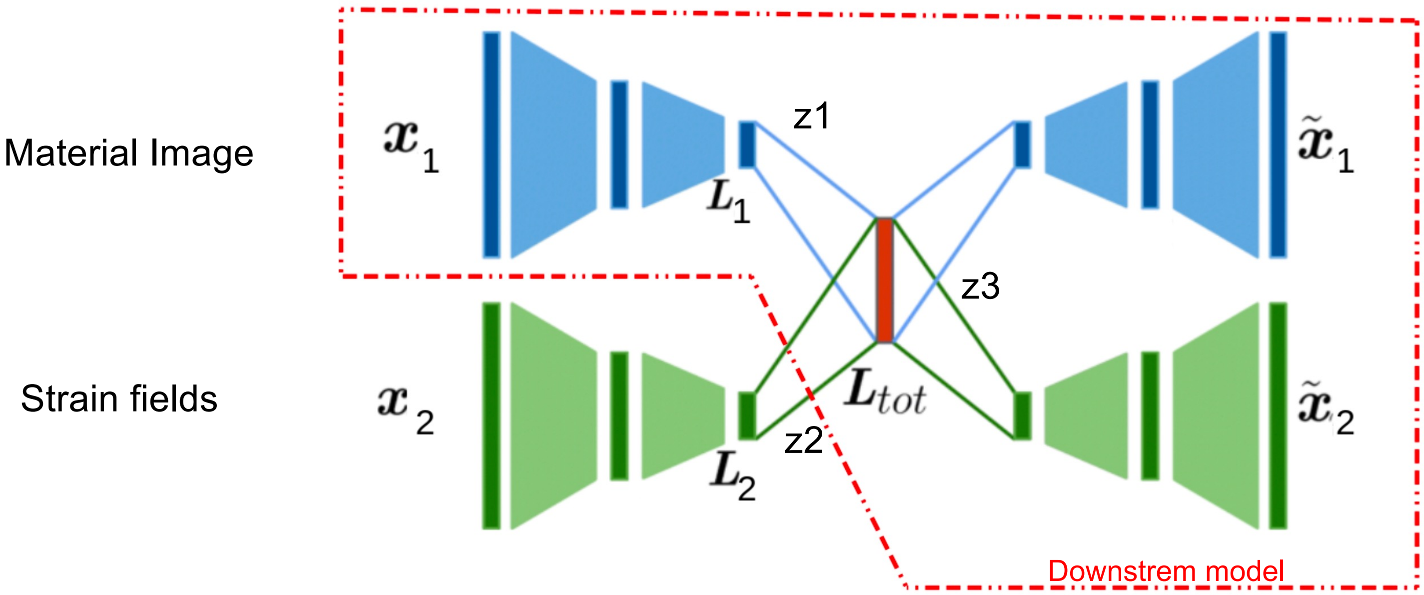

z3 = (z1+z2)/2
z1=z2

H. Launay’s PhD
Th. Gossel

Mechanical autoencoder for strain fields

Train dataset : 3000 strain fields

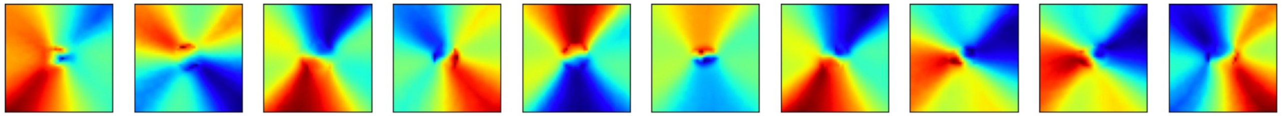

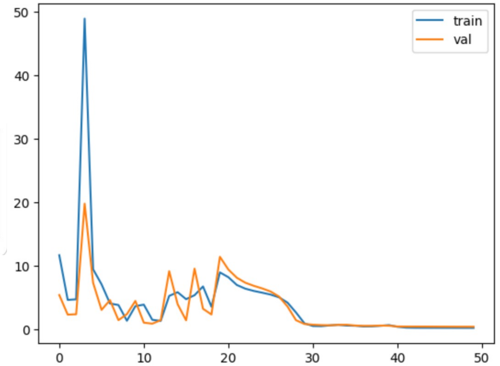

Test

GT

Prev

Error

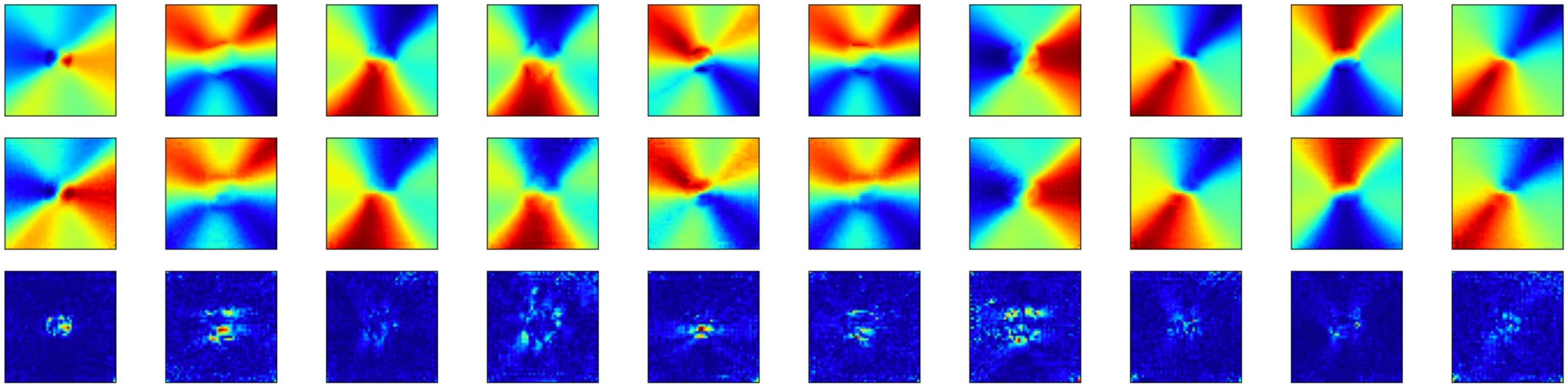

Mechanical autoencoder for strain fields

Map of local mean errors

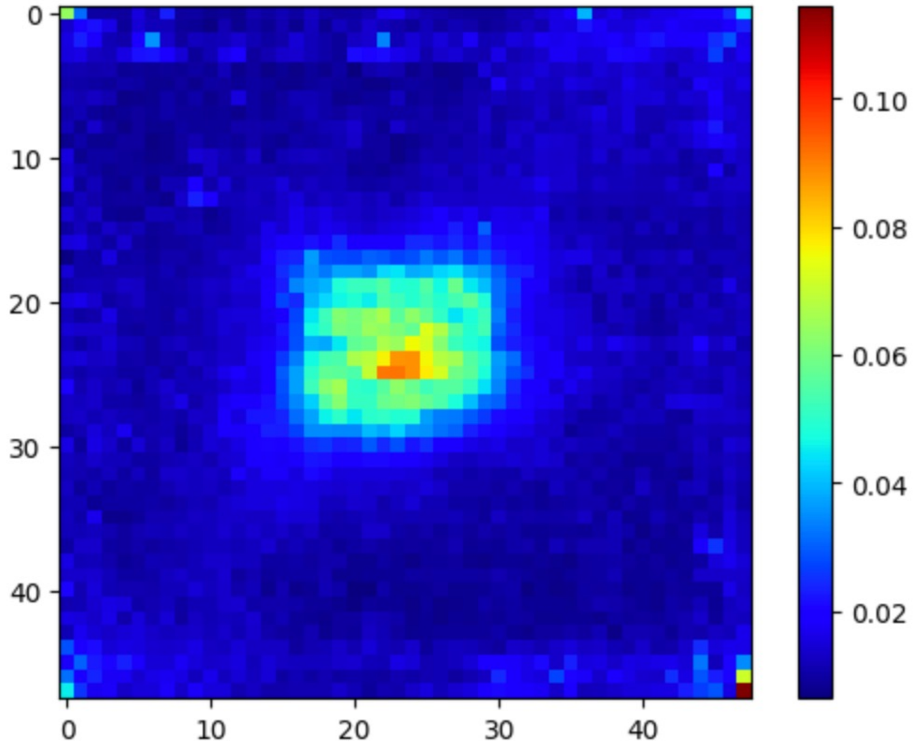

Fully consistent with Saint-Venant’s principle and FE submodeling.

Multimodal autoencoder for FE submodeling using IBC

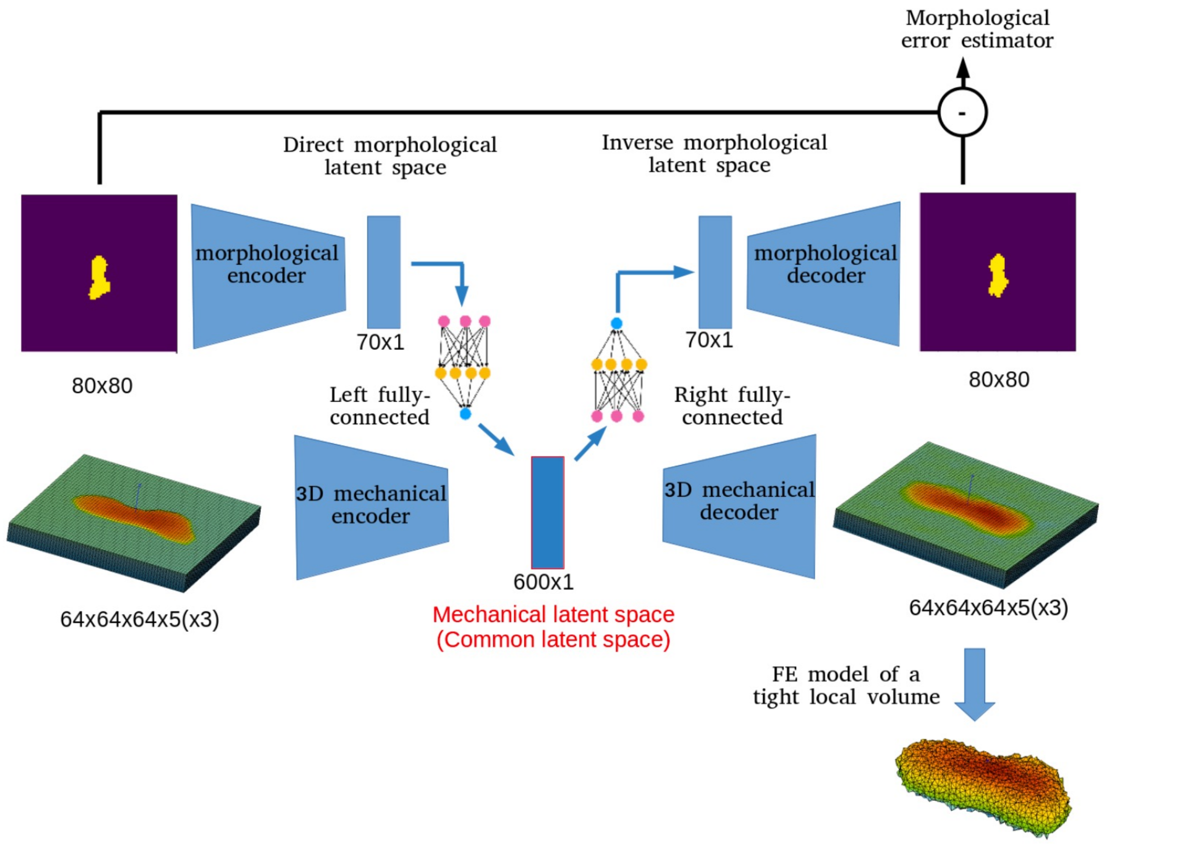

Figure 6: Modified MM Capture d'écran d error indicator to generate displacement field on TLV.

H. Launay's PhD

Multimodal autoencoder for FE submodeling using IBC

3D crack modeling

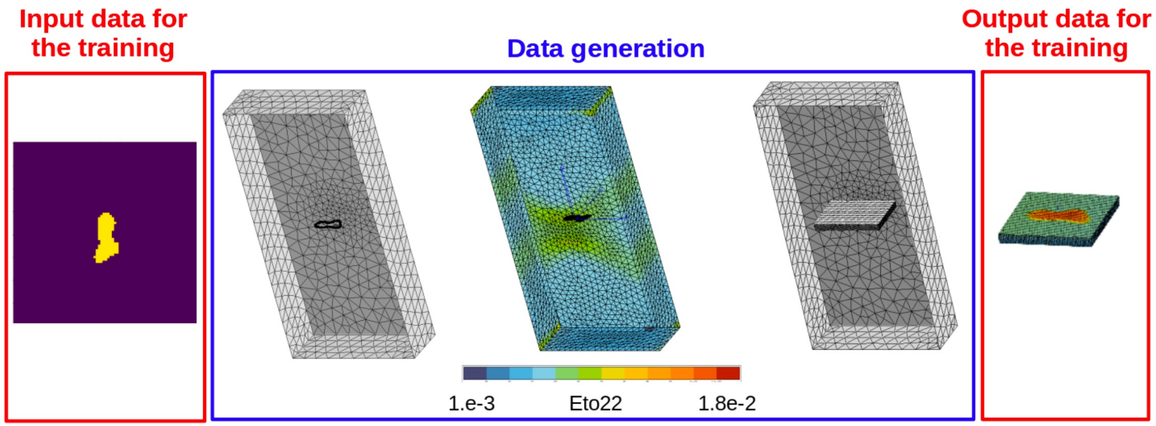

Figure 4: (a) 2D image representing the crack, (b) insertion of the 2D crack in the 3D mesh, (c) $\underset{\sim}{E}_{22}$ field, (d) position of the encoding mesh in the full structure and (e) the encoding mesh with the transferred information.

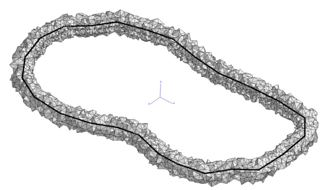

Figure 29: Smaller TLV for defect 1054

Tight local volume
Hybrid model
FE submodel using learned BC.

Multimodal autoencoder for FE submodeling

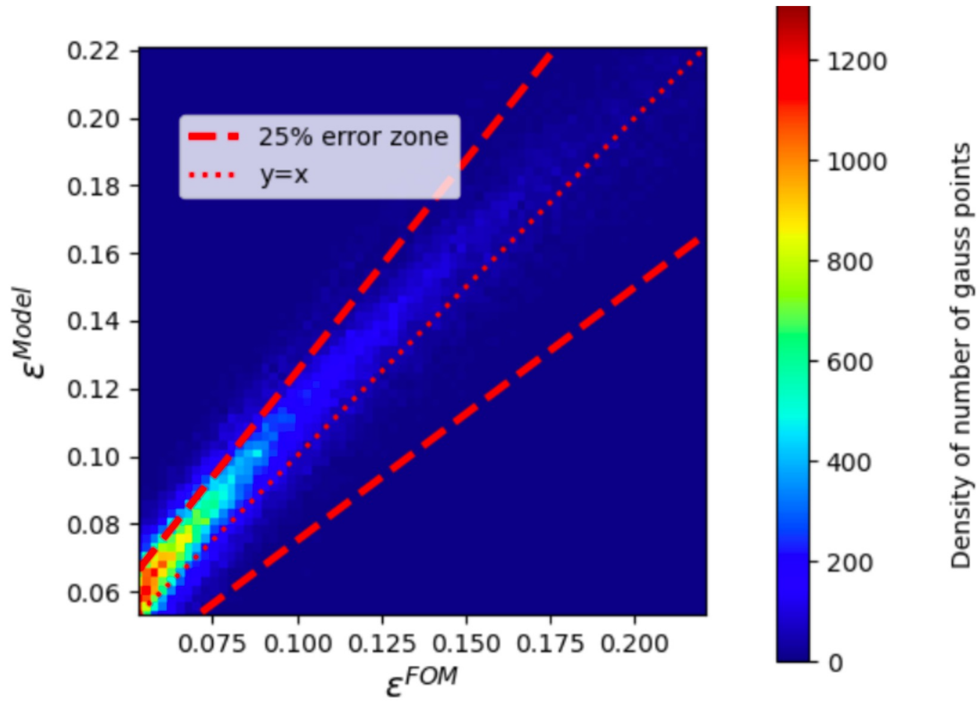

Multimodal autoencoder for FE submodeling

Plasticity, isotropic hardening, speedup = 10

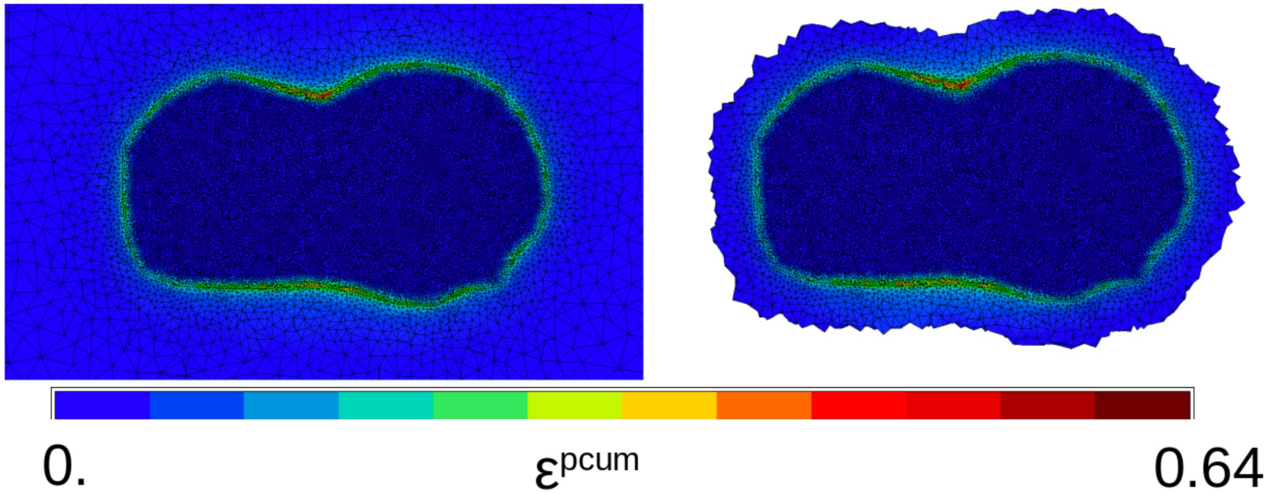

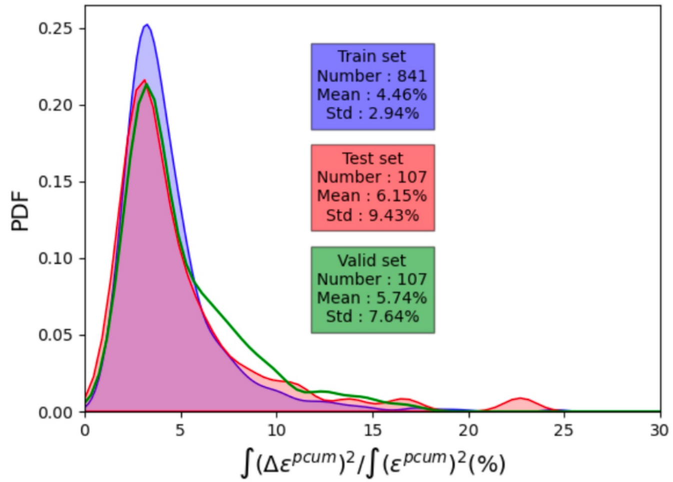

Accuracy versus speedup

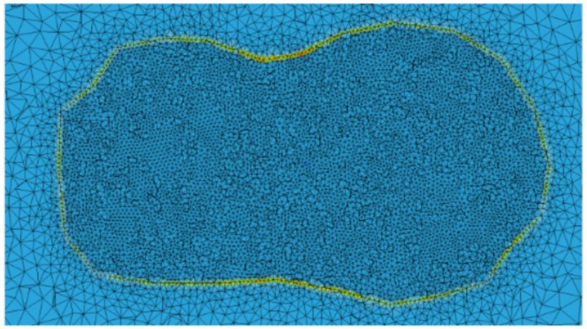

FE submodels using IBC

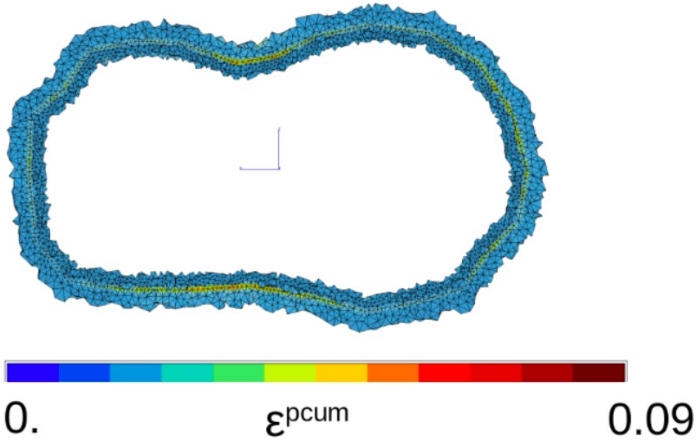

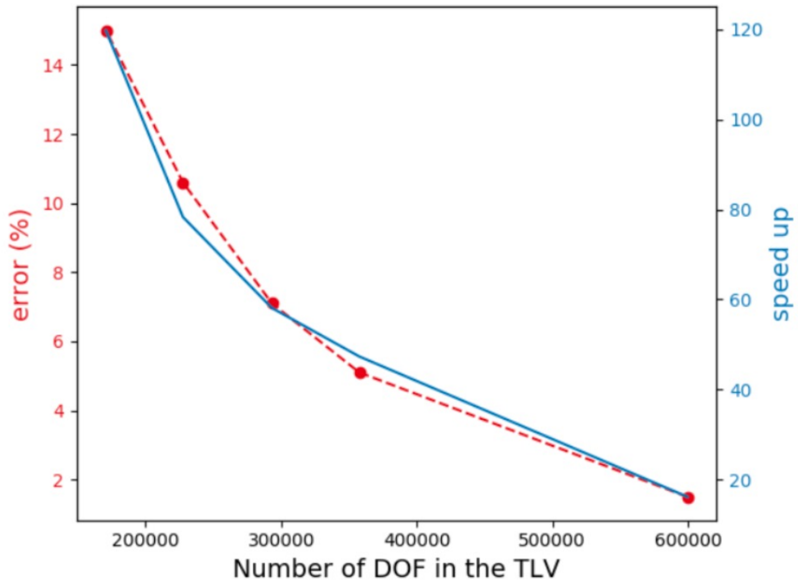

(b)

Toward XAI using FE submodels

Other self-supervised ML : Dictionnary-based ROM-net

Self-supervised learning of a piece-wize linear latent space
Dictionary of local reduced bases, data clustering and a classifier.

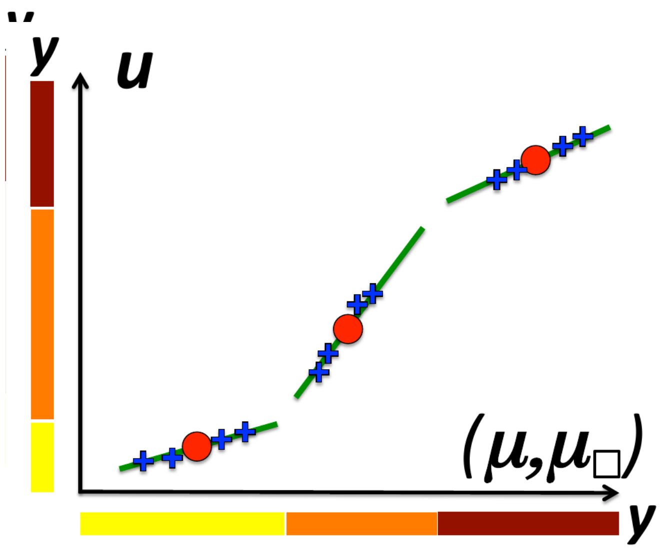

y : computed labels using data clustering and Grassmann distance

Data clustering* using the Grassmann distance between local reduced vector spaces

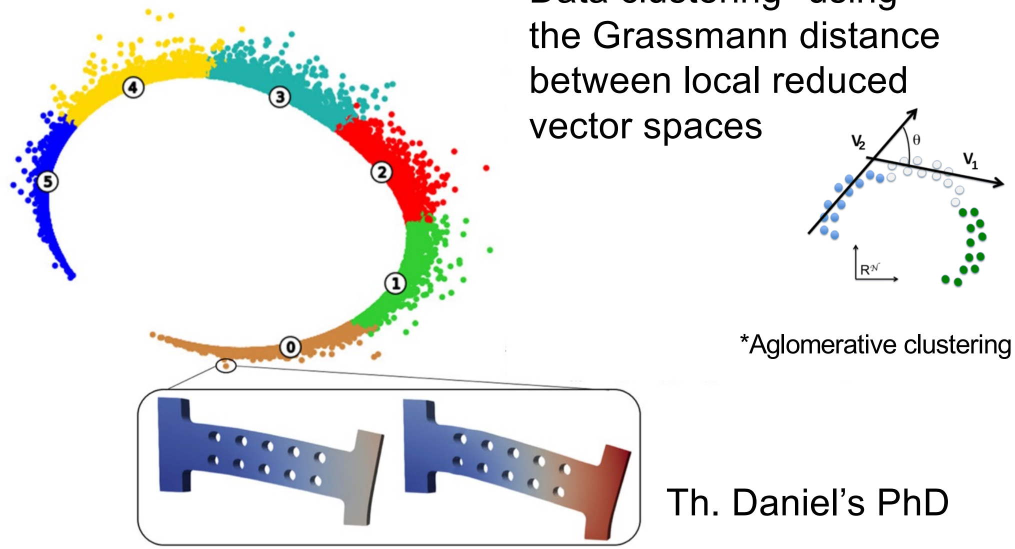

*Aglomerative clustering

Th. Daniel's PhD

Fig. 7 MDS plots of clustering results. The positions of the clusters' labels correspond to the medoids. Each point corresponds to a subspace $\mathcal{V}(T_i)$ spanned by two displacements fields of the simplified mechanical problem with the thermal loading T_i

Dictionnary-based ROM-net using local hyperreduction

Application to welded assembly observed via X-Ray Tomography [L. Lacourt's PhD]

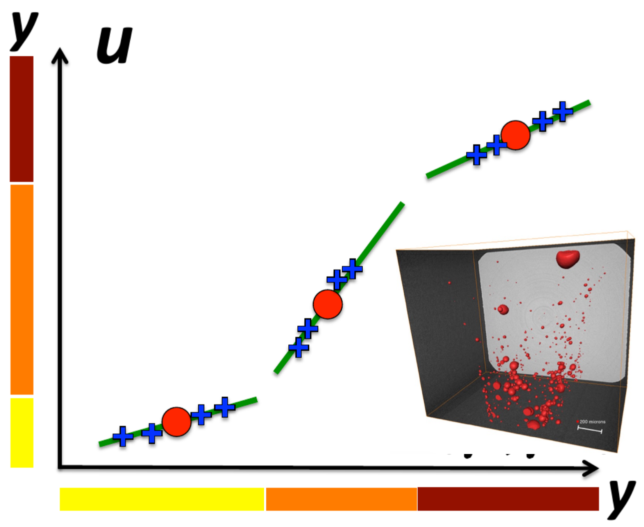

Piece-wize linear latent space of low rank approximation for the training data.

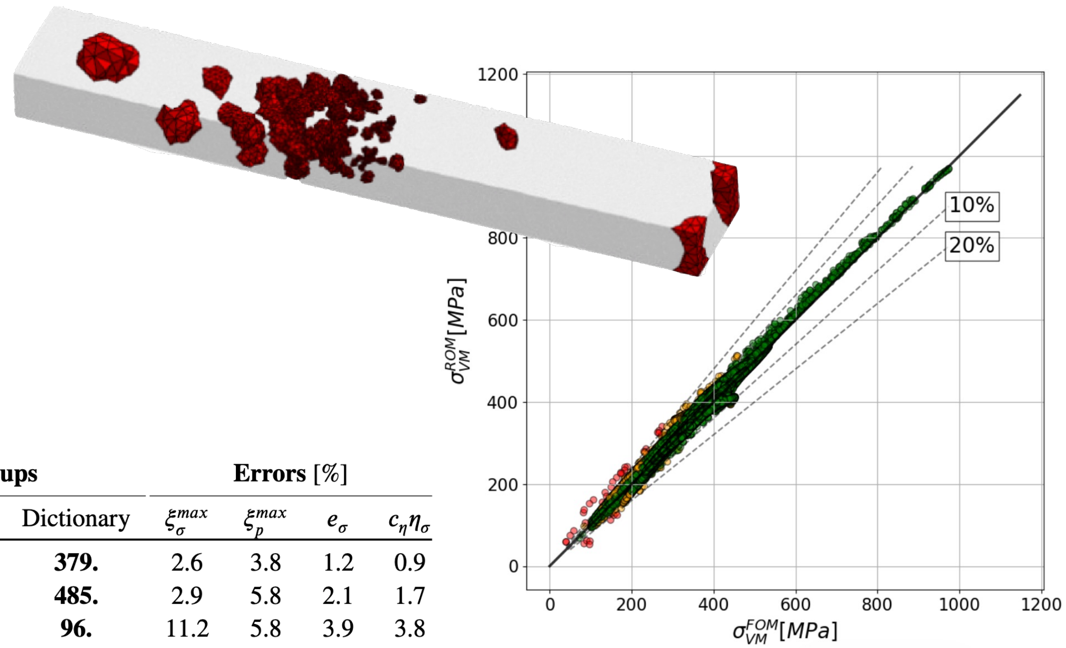

Configuration		Offline phase		Cyclic calculation		Speedups		Errors [%]			
Case	R [mm]	macroscopic	defect	HROM	FOM	No Dictionary	Dictionary	ξ_σ^{max}	ξ_p^{max}	e_σ	$c_\eta \eta_\sigma$
1	0.05	195 s	38 s	25 s	9,480 s	**150.**	**379.**	2.6	3.8	1.2	0.9
2	0.1	195 s	38 s	15 s	7,278 s	**137.**	**485.**	2.9	5.8	2.1	1.7
3	0.25	195 s	38 s	26 s	2,507 s	**39.**	**96.**	11.2	5.8	3.9	3.8
4	0.3	195 s	38 s	27 s	2,197 s	**33.**	**81.**	15.8	4.6	4.6	4.5

Conclusion

Many data représentations: graph (FE mesh), image, tensor and all combination

Many applications :

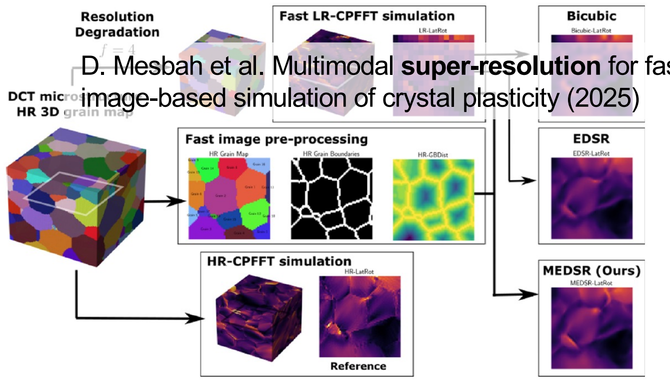

D. Mesbah et al. Multimodal **super-resolution** for fast image-based simulation of crystal plasticity (2025)

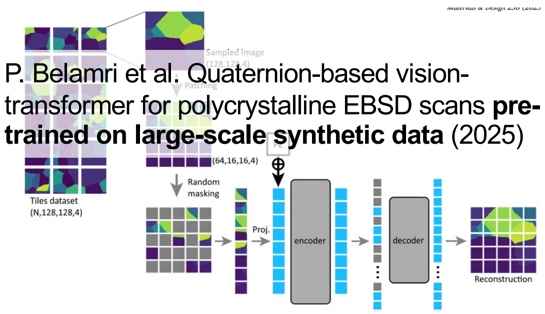

P. Belamri et al. Quaternion-based vision-transformer for polycrystalline EBSD scans **pre-trained on large-scale synthetic data** (2025)

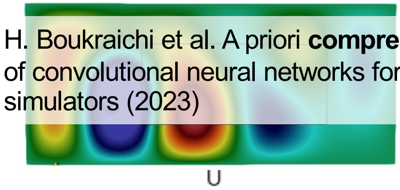

H. Boukraichi et al. A priori **compression** of convolutional neural networks for wave simulators (2023)

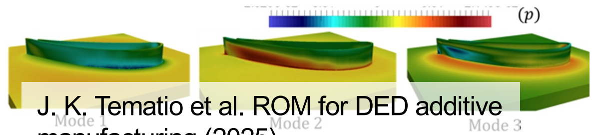

J. K. Tematio et al. ROM for DED additive manufacturing (2025)

N. Akkari et al. A bayesian nonlinear ROM using VAE (2022)

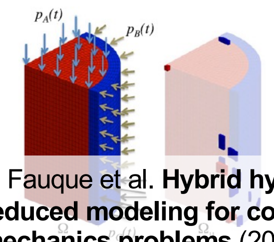

J. Fauque et al. **Hybrid hyper-reduced modeling for contact mechanics problems** (2018)

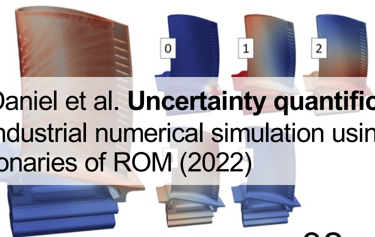

Th Daniel et al. **Uncertainty quantification** for industrial numerical simulation using dictionaries of ROM (2022)

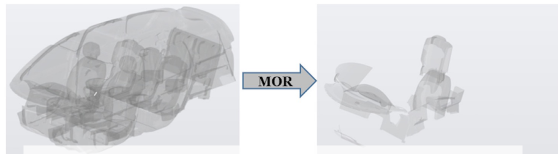

Y. Hammadi et al. Data-driven reduced bond graph for nonlinear multiphysics dynamic systems (2021)